

## Adsorptive removal of phenol from aqueous solutions using chemically activated rice husk ash: equilibrium, kinetic, and thermodynamic studies

Ahmad Jonidi Jafari<sup>a,b</sup>, Ahamd Alahabadi<sup>c</sup>, Mohmmad Hossien Saghi<sup>c</sup>, Zahra Rezaei<sup>c</sup>,  
Ayoob Rastegar<sup>a,c,\*</sup>, Maryam Sahib Zamani<sup>d</sup>, Pardeep Singh<sup>e,f</sup>,  
Ahmad Hosseini-Bandegharai<sup>c,g,\*</sup>

<sup>a</sup>Department of Environmental Health Engineering, School of Public Health, Iran University of Medical Sciences, Tehran, Iran, Tel. +98 5144419572; Fax: +98 5144445648; email: rastegar.89@gmail.com (A. Rastegar), Tel. +98 2186704734; Fax: +98 2186704734; email: ahmad\_jonidi@yahoo.com (A. Jonidi Jafari)

<sup>b</sup>Research Center for Environmental Health Technology, Iran University of Medical Sciences, Tehran, Iran

<sup>c</sup>Department of Environmental Health Engineering, School of Public Health, Sabzevar University of Medical Sciences, Sabzevar, Iran, Tel. +98 5144419572; Fax: +98 5144445648; emails: ahoseinib@yahoo.com (A. Hosseini-Bandegharai), ahmad\_health@yahoo.com (A. Alahabadi), Saghi9@gmail.com (M.H. Saghi), rezaiz41@yahoo.com (Z. Rezaei)

<sup>d</sup>Department of Food and Drug, Iran University of Medical Sciences, Tehran, Iran, Tel. +98 5144419572; Fax: +98 5144445648; email: m.sab2011@yahoo.com

<sup>e</sup>School of Chemistry, Faculty of Basic Sciences, Shoolini University, Solan (HP), India, Tel. +91-1792-308000; Fax: +91-1792-308000; email: pardeepchem@gmail.com

<sup>f</sup>Himalayan Centre for Excellence in Nanotechnology, Shoolini University, Solan (HP) 173229, India

<sup>g</sup>Department of Engineering, Kashmar Branch, Islamic Azad University, P.O. Box 161, Kashmar, Iran

Received 26 June 2018; Accepted 24 March 2019

### ABSTRACT

Phenol can cause environmental problems due to low biological degradation, high toxicity and long persistence in the environment. Thus, the removal of phenol and its derivatives from water is of great importance. Application of agricultural waste materials has been intensively investigated for many years for adsorptive removal of active pollutants. The objective of this research was to improve the adsorption capacity of rice husk ash by activation with different chemical agents for removing phenol from aqueous solutions. Fourier transform infrared spectroscopy, Brunauer–Emmett–Teller (BET), and field emission electron scanning microscopy techniques were used for characterization, and the modified rice ash husk was compared with the conventional one. Results indicated that the effect of chemical treatment by  $\text{NH}_4\text{Cl}$  was better than the other tested chemical agents. The BET specific surface area of  $\text{NH}_4\text{Cl}$ -activated rice husk ash (ARHA) was  $543 \text{ m}^2/\text{g}$ , and the average pore diameter was  $3.24 \text{ nm}$ . The isotherm and kinetic studies of phenol removal by ARHA showed that the Langmuir model and the pseudo-second-order equation represented the best fit with the adsorption data. The maximum adsorption capacity of phenol onto the newly activated rice husk ash was obtained from the Langmuir isotherm model, which was  $66 \text{ mg/g}$ .

**Keywords:** Adsorption; Rice ash; Activation; Phenol;  $\text{NH}_4\text{Cl}$

### 1. Introduction

Industrial effluents consist of various kinds of contaminants [1,2], such as surfactants, buffers, dyes, phenols,

scouring agents, bleaches, caustic compounds, metals, acids, and xylenes [3], with a wide range of concentration. Among these pollutants, phenol and its derivatives are of the most toxic materials and are widely used in some industries such as coke, tire manufacturing, oil refineries, paper, and plastic industries [4,5]. Phenol can cause environmental

\* Corresponding authors.

problems due to low biologic degradation, high toxicity, and long persistence in the environment [6]. The United States Environmental Protection Agency (USEPA) has categorized the phenol derivatives as high-level contaminants since 1984 and 1 mg/L was considered a permissible level [7]. Phenol levels above 1 mg/L give an unwanted taste and odor to drinking water [8]. The reported dosage of this substance in blood which results in human death is in the range of 4.7–130 mg/L [9].

Therefore, since many industrial effluents contain phenolic compounds [3], it is necessary to identify an effective method for dealing with this problem and, therefore, there is a progressive demand for the removal of phenol and its derivatives from water [10]. The most common methods for removal of phenol and phenolic compounds from aqueous solutions include solvent extraction [10], coagulation [11], advanced oxidation [12], biological degradation [13], membrane filtration [14], photocatalytic degradation [15], electrochemical processes [16], and adsorption [17–19].

However, practical applications of the above-mentioned techniques may be conformed to some drawbacks including high cost, low efficiency, and generation of toxic by-products. Among the techniques offered for removal of phenol, adsorption is the most attractive and effective techniques, due to its high efficiency, low-cost, easy designing, and versatility [20], and has been widely welcomed by environmentalists [5]. Adsorption using bio-sorbents, including agricultural by-products, has been found to be an attractive process for the removal of pollutants, especially organic materials, from industrial effluents [21–24]. In this context, a variety of agricultural by-products, such as cocoa shell [25,26], coconut shell [27], pomegranate peel wastes [28], cashew nut shell [29], orange peel [30], rice husk [31,32], etc., have been used as adsorbent for removal of different contaminants from aqueous solutions. However, the low adsorption capacity of such bio-sorbents has limited their usefulness in the removal of contaminants from water. To overcome this problem, agricultural by-products can be transformed to biochars or activated carbons which are of higher surface area and adsorption capacities [33]. For instance, among the mentioned agricultural wastes mentioned, rice husk has been used as activated carbon to clean the environment from contaminants, because it has been reported as a good adsorbent to remove a lot of contaminants [34]. Rice husk ash (RHA), in conventional or modified form, has shown to be very effective adsorbent in the adsorption of active dyes [35], arsenic [35], heavy metal ions [36], phenol [37], bisphenol [38], phosphate [39], etc. from aqueous solutions.

The adsorption capacity of adsorbents strongly depends on the activation method and the conditions of production [20]. In chemical activation processes and preparation of activated carbons, the adsorbent can be saturated (soaked) with a chemical material and pyrolyzed at a specific temperature [40,41]. By the employment of a beneficial method of activation, surface area and porosity of the adsorbent significantly increase, and functionality is modified, which altogether improve the adsorption properties of the activated carbon toward special pollutants and consequently leads to decreasing the amount of activated carbon consumption [41]. In the present work, in the light of the need for production of new beneficial adsorbents, RHA was exploited

for preparation of a more effective activated adsorbent for phenol removal from aqueous solutions. The principal aim of this work was the investigation of the influence of some chemical agents, including MgO, CaCl<sub>2</sub>, KOH, MgCl<sub>2</sub>, NaOH, NH<sub>4</sub>SO<sub>4</sub>, NH<sub>4</sub>Cl, and ZnCl<sub>2</sub>, in the improvement of adsorption capacity of RHA toward phenol. Furthermore, the effect of different experimental variables on activated rice husk ash (ARHA) adsorption capacity was carefully studied, including solution pH, reaction time, initial phenol concentration, amount of adsorbent, and temperature. Also, light was thrown to the equilibrium, kinetic, and thermodynamic aspects of the adsorption process.

## 2. Materials and methods

This fundamental and applicable scientific research was performed using batch experiments. The materials used in the experiments purchased from Merck (Darmstadt, Germany) company. Solutions of 0.1 M NaOH and 0.1 M HCl were applied for adjustment of pH in the aqueous solutions, using a pH meter (HACH-HQ-USA) for pH measurements. The residual phenol concentrations were measured using a UV-Vis spectrophotometer equipment (CECIL CE7400, England) at 500 nm according to the Standard Methods for the Examination of Water and Wastewater [42].

### 2.1. Characterization of adsorbent

The rice ash husk activated with NH<sub>4</sub>Cl was analyzed for its surface characteristics, using N<sub>2</sub> adsorption at 77 K [43], carried out on a Micromeritics ASAP 2020, (USA). The EDX analysis of the adsorbent (NH<sub>4</sub>Cl-activated RHA; ARHA) was also performed to identify the elements present in the composition of adsorbent, using a MIRA3 TESCAN instrument equipped with an EDX analysis system. The field emission electron scanning microscopy (FESEM) micrographs of the adsorbent were recorded, using MIRA3 TESCAN instrument, before and after phenol adsorption for observing the possible changes in surface morphology of ARHA after adsorption process. Surface functional groups of the NH<sub>4</sub>Cl-activated rice husk before and after phenol adsorption was recorded by Fourier transform infrared spectroscopy (FTIR, PerkinElmer).

### 2.2. Optimization of adsorption capacity of activated rice husk

The applied rice husk in this study was initially obtained from the northern part of Iran. Then, the obtained rice husk was grounded to obtain small pieces (2–5 mm). Afterward, the husks were thoroughly washed with distilled water to remove all dirt and oven-dried at 105°C for 24 h. In order to produce ash, the oven-dried rice husk was heated at 500°C in a muffle furnace for 2 h. Different chemical agents, including MgO, CaCl<sub>2</sub>, KOH, MgCl<sub>2</sub>, NaOH, NH<sub>4</sub>SO<sub>4</sub>, NH<sub>4</sub>Cl, and ZnCl<sub>2</sub>, were used for activation and enhancement of the adsorption capacity of RHA. To check the effect of each of activation agent separately, a 5% (w/v) solution of that agent was added to a 250 mL Erlenmeyer flask. The suspension was stirred using a shaker at 100 rpm for 2 h, followed by drying in an oven at 105°C. Finally, the activation of impregnated ash was done at an average temperature of

800°C for 2 h under  $N_2$  gas. Then, the prepared adsorbent was repeatedly washed several times with distilled water to remove all impurities and was dried in an oven at 105°C. In order to select the most suitable activating agent, the adsorption experiments were carried out. Afterward, the effect of weight ratio of the selected activation agent (0%–20%) was investigated to find the best weight ratio for reaching the highest removal efficiency.

### 2.3. Experimental

Analytical reagent grade phenol (purity > 98%) was used in all experiments, and all phenol solutions were prepared in laboratory conditions. The stock solution was obtained by dissolving 1 g phenol in 1 L of double distilled water. The applied phenol solutions for adsorption experiments were prepared by serial dilution of the stock solution. Adsorption studies of phenol on ARHA by different chemical reagents were conducted in batch conditions. In this study, the effect of five variables, that is, ARHA dosage (0.05, 0.1, 0.15, and 0.2 g per 50 mL), contact time (2, 5, 10, 20, 40, 60, 80, and 100 min), solution pH (3–11), initial pollutant concentrations (50–300 mg/L) and temperature (20°C, 30°C, and 50°C) was investigated. In order to investigate the effect of each factor and to optimize it, that factor was continuously changed, and the others were fixed at a specified value. In order to mix the adsorbate and adsorbent completely, the contents were shaken thoroughly using a mechanical shaker rotating with a speed of 200 rpm. In the end, isotherms, kinetics, and thermodynamics were studied under the optimum conditions. In general, the adsorption capacity of phenol or the amount of phenol adsorbed per gram of adsorbent  $q_{eq}$  (mg/g) and the adsorption percentage of phenol were calculated using Eqs. (1) and (2) as follows [44]:

$$q_e = \frac{C_0 - C_t}{M} \times V \quad (1)$$

$$R = \frac{C_0 - C_t}{C_0} \times 100 \quad (2)$$

where  $R$  is the adsorption efficiency (%),  $C_0$  is the initial concentration of phenol (mg/L),  $C_t$  is the concentration of phenol in the solution at equilibrium time (mg/L),  $q_e$  is the adsorption capacity (mg/g),  $V$  is the volume of the phenol solution (mL), and  $M$  is the adsorbent dosage (mg).

## 3. Results and discussion

### 3.1. Effects of various activation agents

For finding the influence of each chemical on phenol removal, phenol solution (50 mg/L) was equilibrated with the ARHA samples, prepared by applying a ratio of 5% w/v of activation agent/rice husk ash, at neutral pH and adsorbent dosage of 2 g/L. The obtained data have been summarized in Fig. 1a in which it can be observed that the untreated RHA had a low phenol removal efficiency (57.09%). Fig. 1 reveals that the activation of RHA by different chemicals, especially with those which have ammonium in their structure, increased the removal percentage of phenol, in comparison with untreated RHA. Among the adsorbents produced by using different activation agents, RHA activated with ammonium chloride had the highest efficiency (94.85%) for phenol removal. Ammonium chloride provides more porosity on the adsorbent surface, which can be assigned to its explosion properties at high temperatures [40]. In contrast, some of the other chemicals such as MgO, KOH, ZnCl<sub>2</sub>, CaCl<sub>2</sub>, etc. precipitates on the adsorbent surface, leading to lessening the adsorption sites available on the surface area of adsorbent [45]. The superiority of  $NH_4Cl$ -activated carbon for removal of phenol is consistent with the confirmed high capacity of activated carbons prepared in the presence of ammonium salts as an activation agent [46,47].

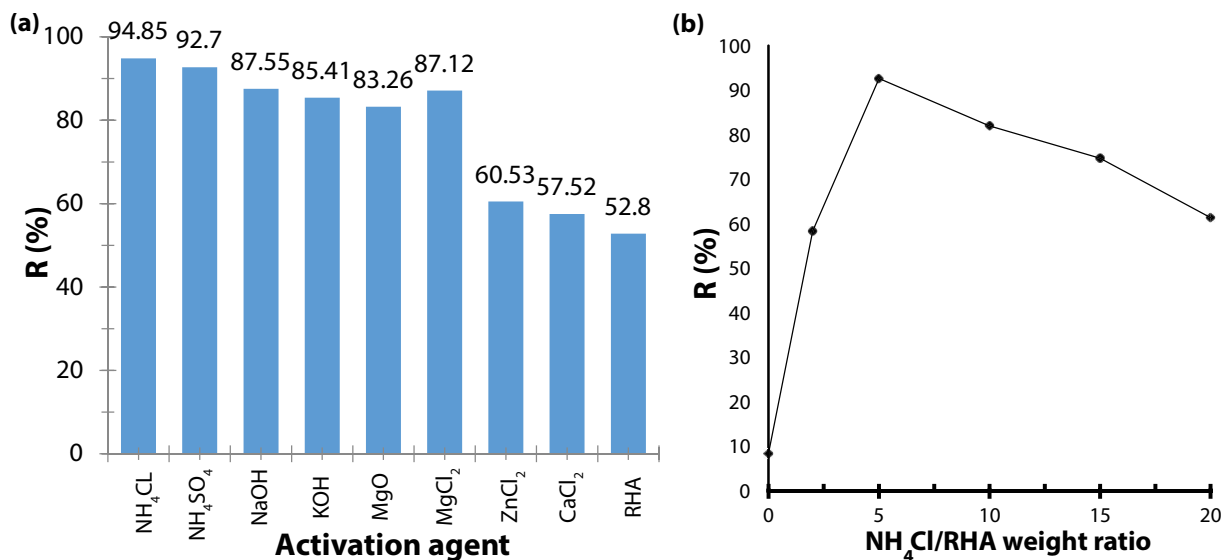


Fig. 1. Effect of different activation agents (a) and weight ratio (w/v) of  $NH_4Cl$ /RHA (b) on the efficiency of phenol removal by  $NH_4Cl$ -activated RHA (ARHA).

To investigate the effect of weight ratio (w/v) of the most suitable activation agent, that is, ammonium chloride, various amounts of this agent were used for activation of RHA. Results (Fig. 1b) indicated that the adsorption efficiency of phenol increased with increasing ammonium chloride concentration from 2% to 5% and decreased at  $\text{NH}_4\text{Cl} > 5\%$ . It seems that ammonium chloride/RHA weight ratios lower than 5% lead to lesser porosity and, hence, lower surface areas and lower phenol adsorption capacities. On the other hand, ammonium chloride/RHA weight ratios higher than 5% lead to activated RHA samples in which the developed pores become too wide and, due to the creation of fewer micropores and mesopores, the surface areas of the samples and their adsorption capacity toward phenol become lower.

### 3.2. Adsorbent characterization

The isotherm of  $\text{N}_2$  adsorption–desorption for both the prepared adsorbent (ARHA) and its parent rice husk ash (RHA) can be observed in Fig. 2, along with the pore size distribution curves. Also, Table 1 shows the specific surface area and other features of both ARHA and RHA. The results indicate that the specific surface area Brunauer–Emmett–Teller (BET), pore size, and pore volume of the adsorbent are, respectively, equal to  $543.7 \text{ m}^2/\text{g}$ ,  $3.24 \text{ nm}$ , and  $0.44 \text{ cm}^3/\text{g}$  and are completely different from those of the parent RHA which are  $17.7 \text{ m}^2/\text{g}$ ,  $31.66 \text{ nm}$ , and  $0.14 \text{ cm}^3/\text{g}$ , respectively. According to the International Union of Pure and Applied Chemistry (IUPAC), the values of average pore diameter (i.e.,  $3.24$  and  $31.66 \text{ nm}$ ) indicate that both the newly prepared

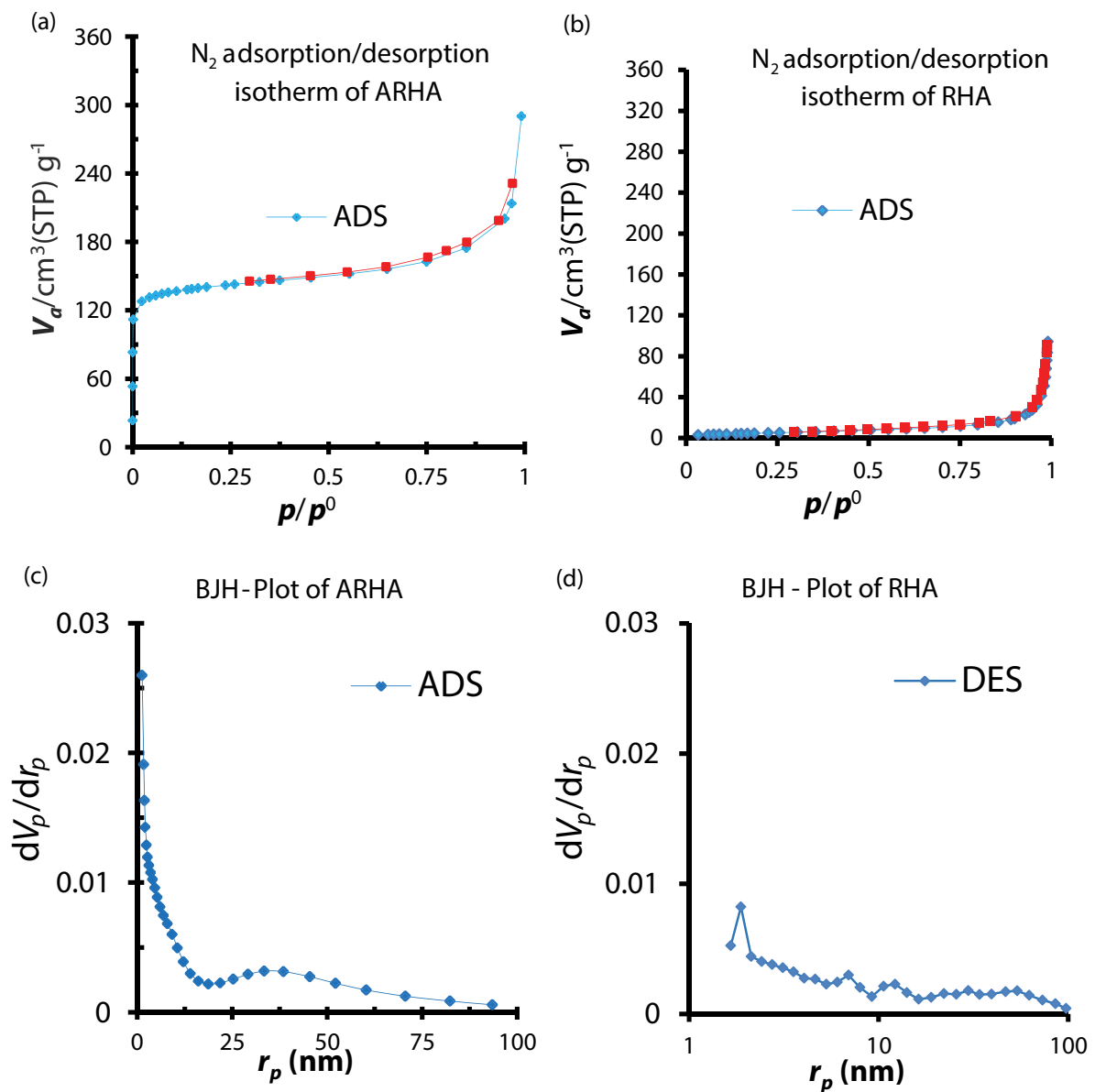


Fig. 2. Comparison of  $\text{N}_2$  adsorption and desorption isotherms (a and b) and BJH plots (c and d) of rice husk ash (RHA) and  $\text{NH}_4\text{Cl}$ -activated RHA (ARHA).

Table 1  
Special surface and other characteristics of rice husk ash (RHA) and  $\text{NH}_4\text{Cl}$ -activated RHA (ARHA)

Parameter	Magnitude	
	RHA	ARHA
BET surface area, $\text{m}^2/\text{g}$	17.7	543.7
Total pore volume, $\text{cm}^3/\text{g}$	0.14	0.44
Monolayer volume, $\text{cm}^3/\text{g}$	4.1	124.9
Average pore size, nm	31.66	3.24
C	52.4	203.7

adsorbent and its parent rice husk ash are of a mesoporous structure. However, in fact, the value of average pore diameter in ARHA is almost one-tenth of its value in RHA, indicating that activation with  $\text{NH}_4\text{Cl}$  develops many small pores in the structure of rice husk ash. The developed pores in ARHA have brought about a much higher surface area and, consequently, a much higher phenol adsorption capacity, compared with pristine RHA.

Additionally, EDX analysis of the new adsorbent ( $\text{NH}_4\text{Cl}$ /RHA) was recorded, and the results can be observed in Fig. 3. The EDX analysis showed a big peak related to the Si element, which is the characteristic of RHA-based adsorbents.

The functional groups of the prepared ARHA were assessed before and after phenol adsorption, using the FTIR (Fig. 4). The FTIR spectra of ARHA, both before and after phenol adsorption, show some remarkable peaks which are related to functional groups of C=C ( $1,515\text{ cm}^{-1}$ ) and silica functional groups of Si-OH ( $3,500\text{--}3,750\text{ cm}^{-1}$ ), Si-O-Si ( $1,080\text{ cm}^{-1}$ ), and Si-H ( $798\text{ cm}^{-1}$ ) [48]. Also, the FTIR spectrum of the adsorbent after phenol adsorption shows an extra peak at  $1,647\text{ cm}^{-1}$  which can be attributed to the cyclic C=C bond of phenol molecules adsorbed on the surface of ARHA.

FESEM micrographs are usually used as a valuable tool to study the surface morphology of adsorbents before after adsorption process. Fig. 5 shows the morphological

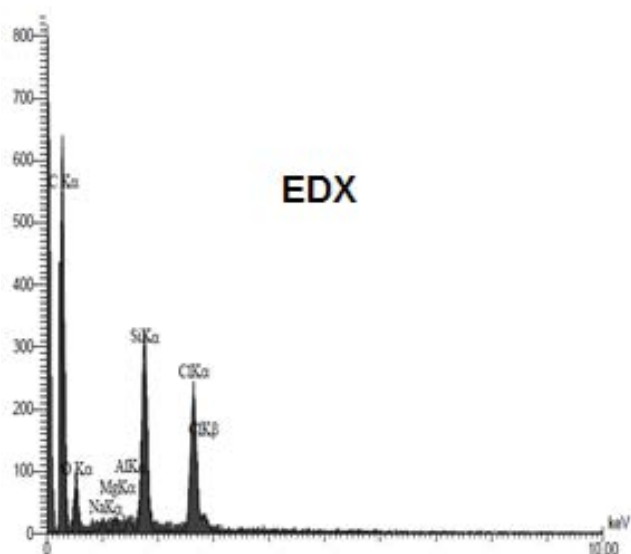


Fig. 3. EDX analysis of modified RHA with  $\text{NH}_4\text{Cl}$ .

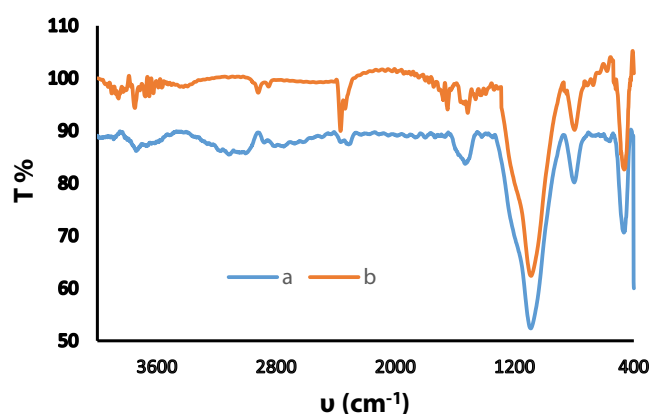


Fig. 4. FTIR spectra of  $\text{NH}_4\text{Cl}$ -activated rice husk ash (ARHA) before (curve a) and after (curve b) phenol adsorption.

characteristics of pristine RHA adsorbent, along with those of ARHA adsorbent before and after phenol adsorption. The figure shows that the ARHA contains well developed, non-uniform cavities which are very helpful for adsorption of phenol to the interior surface of the adsorbent. Such well-developed cavities could be due to the explosion property of ammonium chloride at high temperatures, which also is responsible for the high specific surface area of the fabricated adsorbent. However, comparing the FESEM micrographs does not reveal any morphological change in the surface of the adsorbent due to occurring the adsorption process.

### 3.3. Effect of pH and contact time on phenol removal

Solution pH is a critical experimental factor which has a significant influence on phenol removal, due to altering adsorbent charges, ionization degree, and enhancement of functional groups on surface active binding sites and also solution chemistry [49]. The effect of pH in the range 3–11 for the removal of phenol by ARH was tested in the contact time 5–100 min. It can be seen from Fig. 6a that from pH 3.0 to 5 the rate of the removal of phenol increased but then with the further increase of pH 7–11 decreased. Also, the phenol removal efficiency increased with increasing the contact time, and an almost maximum removal percentage (93.13%) occurred within the first 15 min of adsorption and the equilibrium state was attained within 60 min. Under the equilibrium conditions, maximum phenol removal efficiency was obtained to be 97.93%. Therefore, optimum adsorption conditions of phenol were obtained at pH 5 and 60 min of contact time. The experimental results revealed that the isoelectric point ( $\text{pH}_{\text{zpc}}$ ) for ARHA was 5.8. At pH values close to  $\text{pH}_{\text{zpc}}$  of the adsorbent, the ARHA surface is not protonated very much and let the stronger and more rapid physical interactions, such as  $\pi\text{--}\pi$  electron donor–acceptor interactions, to be established between the adsorbent surface and phenol molecules, which lead to further increase of phenol uptake. At low pHs, the surface of the adsorbent is occupied with  $\text{H}^+$  ions which compete with phenol adsorption and reduce its removal percentage. The phenol  $\text{pK}_a$  is 9.95 and, therefore, it dissociates at high pHs. On the other hand, at high pHs, the surface charge becomes negative which results in repulsion between the negatively charged surface and



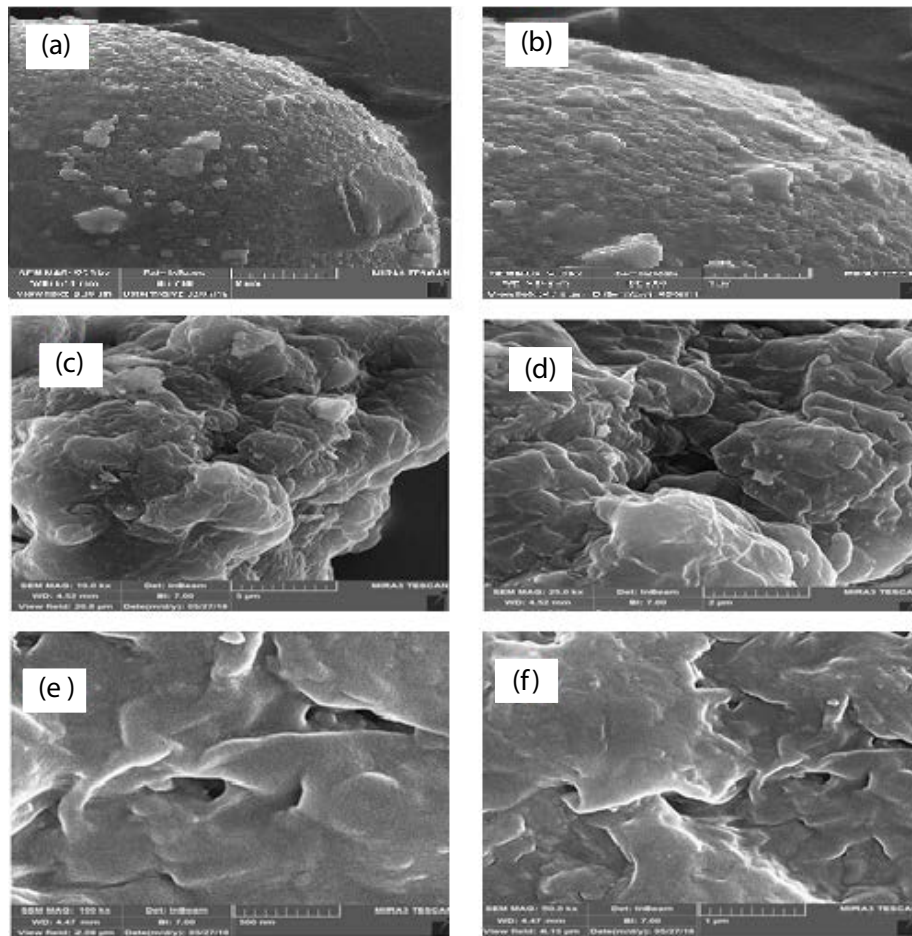


Fig. 5. FESEM of RHA ((a) and (b)), and those of ARHA before ((c) and (d)) and after phenol adsorption ((e) and (f)).

dissociated phenol molecules in the solution, which causes a decrease in the removal efficiency. Also, at basic pH values,  $\text{OH}^-$  competes with phenol adsorption onto the adsorption sites [5]. Anyway, pH 5 was selected for further studies.

#### 3.4. Effect of adsorbent dosage on the removal efficiency at different contact times

Fig. 6b shows the effect of adsorbent dosage on the removal efficiency of phenol. According to this figure, phenol removal efficiency increased with increasing adsorbent dosage from 0.1 to 0.5 g/L, so that, in the early times (5 min), the removal efficiency of phenol was increased from 33% to 70.6% with increasing the ARHA dose which might be due to the availability of more adsorption sites. The result showed that phenol adsorption onto the mass unit of adsorbent decreases as the amount of adsorbent dose increases. These results were in accordance with those reported by Mohammadi et al. [10] that mentioned the lack of the available vacant sites as the reason for this adsorption capacity decrease.

#### 3.5. Effect of temperature on the adsorption of phenol

Effect of various temperatures (20°C, 30°C, and 50°C) on the adsorption of phenol by ARHA showed that the removal efficiency improved with an enhancement in

temperature (Fig. 7). It can be seen that, with the increase in temperature from 20°C to 50°C, the rate removal of phenol increased from 87% to >98%. The increase in removal percentage with the increase in temperature was due to the increase in solubility of phenol and the increase of effective collisions between the phenol and adsorption sites in ARHA surface. Also, increasing adsorption percentage at higher temperatures shows that the adsorption process is endothermic and, therefore, the removal process is more favorable at higher temperatures.

#### 3.6. Adsorption kinetics

Adsorption kinetic study is usually employed to assist the understanding of adsorption mechanisms and evaluation of the adsorbent performance [50,51]. Pseudo-first-order and pseudo-second-order models were applied for the estimation of the adsorption kinetics [51]. Pseudo-first-order model and the pseudo-second-order model are expressed in a linear form in Eqs. (3) and (4), respectively, as follows:

$$\ln(q_e - q_t) = \ln q_e - k_1 t \quad (3)$$

$$\frac{t}{q_t} = \frac{1}{k_2 q_e^2} + \frac{t}{q_e} \quad (4)$$

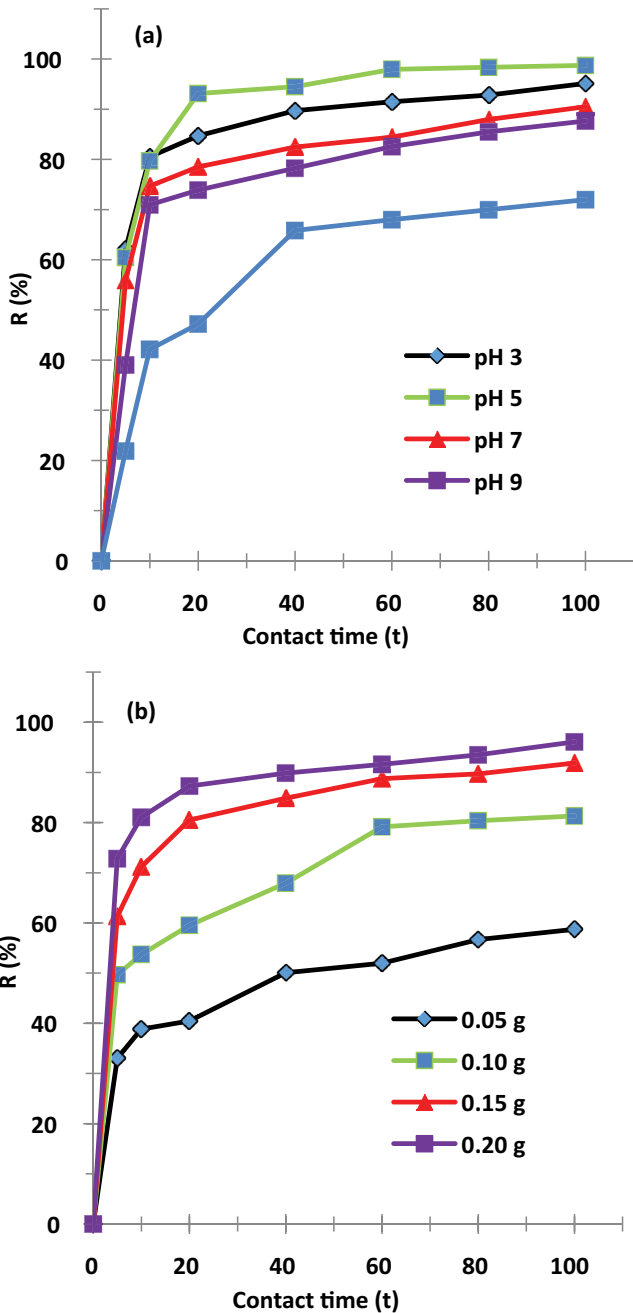


Fig. 6. Effect of pH (a) and adsorbent dose (b) on the removal efficiency of ARHA (phenol concentration = 50 mg/L, and temperature = 293 K).

where  $k_1$  and  $k_2$ , respectively, represent the first-order and the second-order rate constants,  $q_t$  is the adsorption capacity of the adsorbent at time  $t$ , and  $q_e$  is the adsorption capacity at equilibrium [51].

Table 2 and Fig. 8 show the calculated adsorption parameters of phenol removal for the pseudo-first-order and the pseudo-second-order models. According to the results of correlation coefficients for both kinetic models, it can be ascertained that the adsorption kinetics of phenol followed the pseudo-second-order model with relatively high correlation coefficients at all concentration studied.

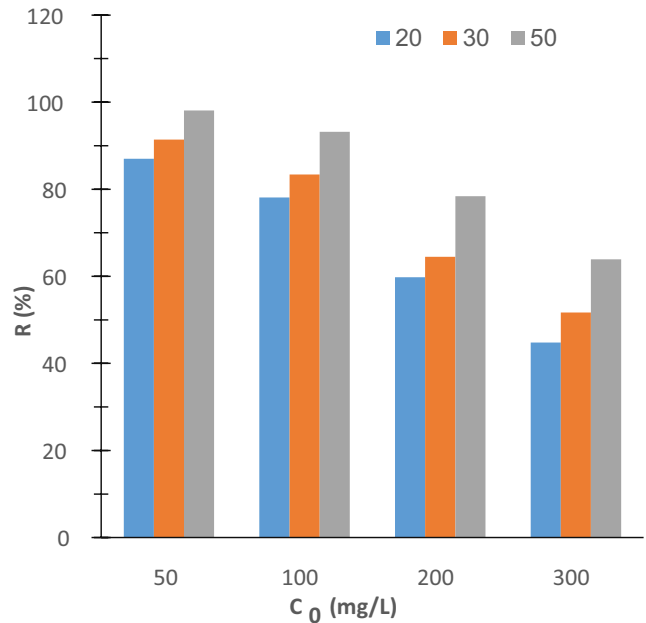


Fig. 7. Effect of temperature on the removal efficiency phenol (phenol concentration = 50 mg/L, adsorbent dose = 1.5 g/L, and pH = 5).

### 3.7. Isotherms of phenol adsorption

Adsorption isotherms are based on the adsorption features and equilibrium data which describe the interaction type of contaminant molecules with the adsorbent materials and play an important role in the optimization of adsorbent consumption. Freundlich and Langmuir models were applied for fitting with the experimental data. The basis of Langmuir model is that the energy of adsorption is stable and the process of adsorption happens on homogeneous surfaces via monolayer adsorption [52,53]. The linear equation of Langmuir model can be presented as below:

$$\frac{C_e}{q_e} = \frac{1}{bq_{\max}} + \frac{C_e}{q_{\max}} \quad (5)$$

where  $q_e$  (mg/g) is the quantity of adsorbate adsorbed at equilibrium,  $C_e$  (mg/L) is the concentration of adsorbate in the equilibrium state,  $b$  (L/mg) is the Langmuir constant,  $q_{\max}$  (mg/g) is the maximum adsorption capacity. The values of  $q_{\max}$  and  $b$  can be calculated via linear plots of  $C_e/q_e$  vs.  $C_e$  [54,55]. The essential characteristics of the Langmuir model can be expressed by a constant called separation factor,  $R_L$ , describing the sorption capability of the adsorbent and is given in Eq. (6).

$$R_L = \frac{1}{1 + bC_0} \quad (6)$$

where  $C_0$  (mg/g) is the initial phenol concentration (mg/L).  $R_L$  value determines the type of the isotherm to be whether favorable ( $0 < R_L < 1$ ), unfavorable ( $R_L > 1$ ), linear ( $R_L = 1$ ), or irreversible ( $R_L = 0$ ). Freundlich equation, unlike the Langmuir model, is an empirical model that considers heterogeneous

and multilayer adsorption of solute onto the adsorbent surface. The linearized form of the Freundlich's equation is expressed as follows:

$$\ln q_e = \ln K_F + \frac{1}{n} + \ln C_e \tag{7}$$

where  $K_F$  and  $n$  are Freundlich constants related to adsorption capacity ((mg/g) (L/mg)<sup>1/n</sup>) and adsorption intensity, respectively. Values of  $1 > n$ ,  $1-2$ , and  $2-10$  represent weak, favorable, and good adsorption conditions, respectively. A plot of

$\ln q_e$  vs,  $\ln C_e$  would give  $n$  and  $K_F$  from the slope and intercept, respectively [41]. Linear isotherms of the Langmuir and Freundlich models are shown in Fig. 9, and the calculated parameters are reported in Table 3.

As can be observed, the adsorption capacity was increased with an increase in temperature from 20°C to 50°C for both Langmuir and Freundlich isotherms, and maximum adsorption capacity in Langmuir model increased from 50 to 66.6 mg/g. According to the obtained correlation coefficients obtained for Langmuir and Freundlich models (Table 2), the adsorption of phenol on ARHA is best-fitted

Table 2  
Values of kinetic parameters for adsorption of phenol onto ARHA surface

Initial phenol concentration $C_0$ (mg/L)	Pseudo-first-order model			Pseudo-second-order model		
	$q_e$	$K_1$	$R^2$	$q_e$	$K_2$	$R^2$
50	4.85	0.034	0.968	15.87	0.018	0.999
100	7.63	0.029	0.943	27.77	0.01	0.999
200	13.05	0.03	0.949	41.66	0.001	0.980
300	13.02	0.033	0.857	43.47	0.006	0.998

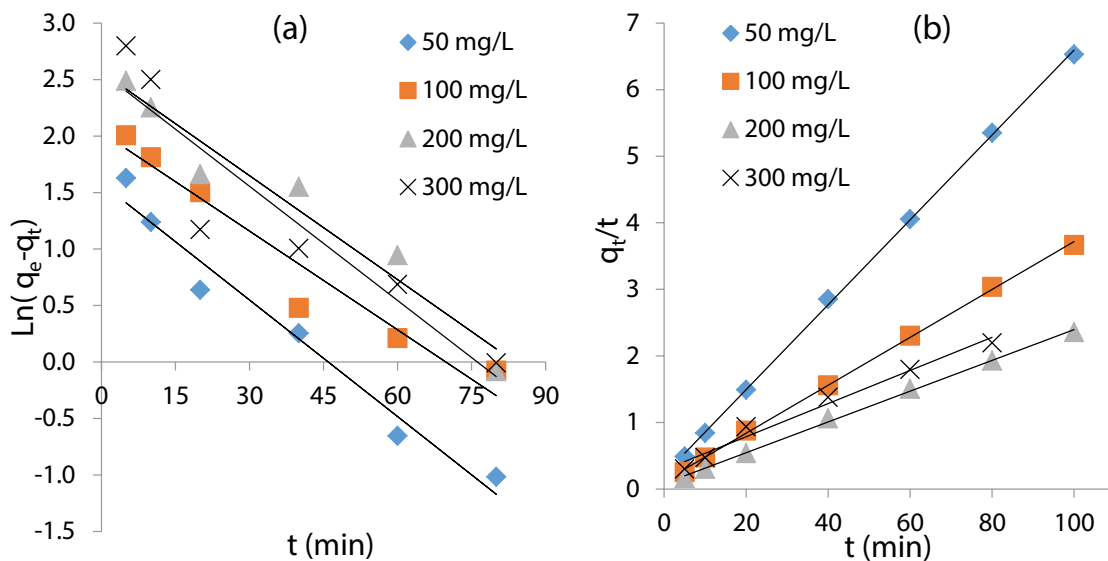


Fig. 8. Pseudo-first-order model (a) and pseudo-second-order model (b) fits of experimental data for phenol adsorption by ARHA adsorbent.

Table 3  
Langmuir and Freundlich isotherm constants of phenol adsorption on ARHA treated

Temperature (K)	Langmuir isotherm				Freundlich isotherm		
	$q_m$	$b$	$R_L$	$R^2$	$n$	$K_F$	$R^2$
293	50	0.05	0.26	0.999	3.46	17.08	0.995
303	58.82	0.06	0.24	0.994	2.92	9.76	0.985
323	66.6	0.14	0.12	0.993	2.84	8.04	0.971



with Langmuir model. This result indicates that phenol adsorption takes place at homogenous adsorption sites and a monolayer adsorption occurs onto the adsorbent surface [45]. The essential characteristic of the Langmuir model is the separation factor,  $R_L$ , describing the adsorption capability of the adsorbent. The results of equilibrium studies showed that the values of  $R_L$  in the present investigation were found to be in the range of 0–1, suggesting that the conditions are favorable for adsorption process [47].

Gholizadeh et al. [56] reported that the maximum adsorption capacity of inactivated rice husk ash was 5.9 mg/g. Higher values of ARHA adsorption capacity for phenol removal would be ascribed to the higher surface area obtained by the application of ammonium chloride as the activation agent.

### 3.8. Thermodynamic studies

Thermodynamic parameters of adsorption give some insight into the process of adsorption, such as whether the nature of the adsorption process is endothermic or exothermic and the process is either spontaneous or not [52]. Unfortunately, in the past decades, many erroneous ways have been utilized for the thermodynamic study of adsorption processes [57,58]. In order to investigate the thermodynamic aspects of ARHA adsorption, the most correct way for calculating thermodynamic parameters, that is, free energy change ( $\Delta G$ ), enthalpy change ( $\Delta H$ ), and entropy change ( $\Delta S$ , is to compute the suitable thermodynamic equilibrium constant ( $K_e^\circ$ ; dimensionless) at any temperature from the isothermal studies using the following equation [59]:

$$K_e^\circ = \frac{(1,000 \text{ Kg molecular weight of adsorbate}) \times [\text{Adsorbate}]^\circ}{\gamma} \quad (8)$$

where  $K_e^\circ$  is the dimensionless thermodynamic equilibrium constant,  $K_g$  (L/mg) is the best-fitted isotherm constant obtained from the isothermal studies at any specified temperature,  $g$  is the coefficient of activity of adsorbate (dimensionless) which can be considered as unity when the solution is sufficiently diluted, or the concentration of ionic compounds is low [60], and  $[\text{Adsorbate}]^\circ$  is the standard concentration of the adsorbate, that by definition is 1 mol L<sup>-1</sup> [61]. Then, van't Hoff equation can be employed for the calculation of thermodynamic parameters using the following equation [59]:

$$\Delta G^\circ = -RT \ln(K_e^\circ) \quad (9)$$

where  $R$  is the universal gas constant (8.314 J K<sup>-1</sup> mol<sup>-1</sup>), and  $T$  is the temperature (K). Considering the 3rd principles of the Thermodynamics, one has the following relation:

$$\Delta G^\circ = \Delta H^\circ - T\Delta S^\circ \quad (10)$$

Combining Eqs. (9) and (10) leads to Eq. (11).

$$\ln(K) = \frac{-\Delta H^\circ}{R} \times \frac{1}{T} + \frac{\Delta S^\circ}{R} \quad (11)$$

By plotting of  $\ln(K_e^\circ)$  vs.  $1/T$ , the changes in  $\Delta S^\circ$  and  $\Delta H^\circ$  can be computed from the intercept the slope, respectively [59,60].

Therefore, using the values obtained for the Langmuir constant ( $b$ ; L/mg) and calculating the thermodynamic equilibrium constants at different temperatures, Fig. 10 was constructed based on Eq. (11), and the thermodynamic parameters were calculated and reported in Table 4. The value of free energy change ( $\Delta G^\circ$ ) was negative and increased

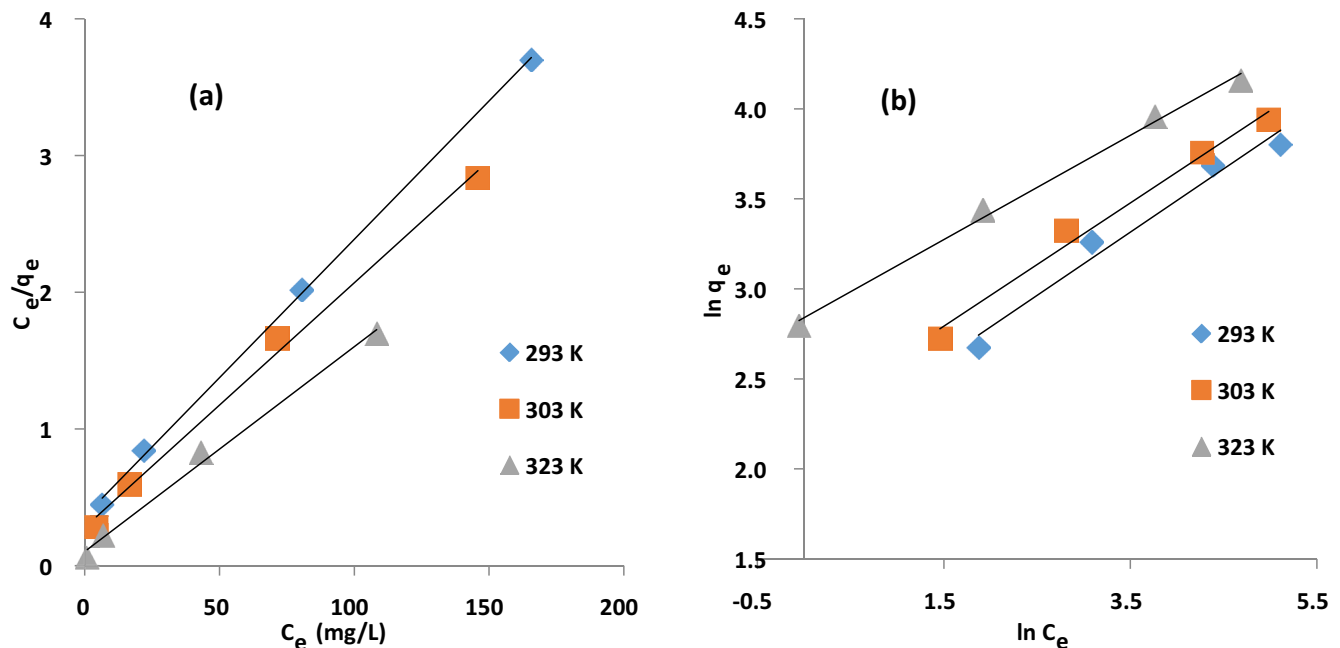


Fig. 9. Adsorption isotherms of Langmuir (a) and Freundlich (b) for phenol adsorption by ARHA.

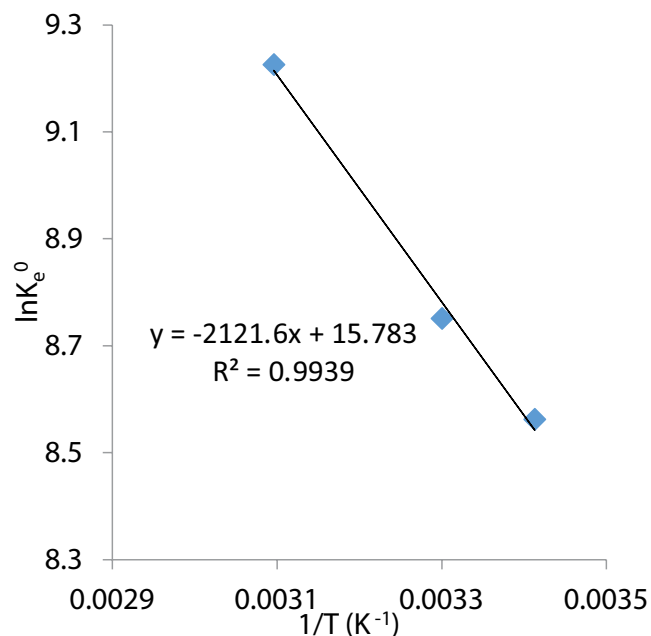


Fig. 10. Thermodynamics of phenol adsorption on ARH treated with  $\text{NH}_4\text{Cl}$ .

Table 4  
Thermodynamic parameters of adsorption of phenol on ARHA

Temperature (K)	$\Delta H^\circ$ (kJ/mol)	$\Delta S^\circ$ (J/mol)	$\Delta G^\circ$ (kJ/mol)
293			-20.86
303	17.64	131.22	-22.04
323			-24.77

with increasing temperature, while the values of enthalpy ( $\Delta H^\circ$ ) and entropy ( $\Delta S^\circ$ ) were positive. Finally, it can be said that the adsorption process exhibited better results at higher temperatures. The positive value of  $\Delta H$  indicates that the adsorption of phenol on ARH is endothermic in nature which is consistent with the effect of temperature on adsorption efficiency. This is due to the strong interaction between adsorbent and phenol [62]. Since the  $\Delta H^\circ$  magnitude for physisorption processes approximately ranges from 2.0 to 20 kJ/mol [63,64], the magnitude of  $\Delta H^\circ$  (17.64 kJ/mol) indicates that the removal process of phenol by ARHA is a physical type of adsorption. The negative values of change in the Gibbs free energy were indicating the spontaneous adsorption of phenol on the adsorbent surface.

#### 4. Conclusion

Results of the present study indicated that chemically activated RHA yielded a better removal efficiency, in comparison with the non-activated one. At similar experimental conditions, the use of different activation agents increased the adsorption capacity for phenol removal. Among the activators tested,  $\text{NH}_4\text{Cl}$  had the highest efficiency and, therefore,  $\text{NH}_4\text{Cl}$ -ARHA was further studied. The results indicated that the activation process with  $\text{NH}_4\text{Cl}$  brings about a much

higher surface area and, consequently, a much higher phenol adsorption capacity for ARHA, compared with pristine RHA. Batch adsorption experiments were performed to throw light on the properties of ARHA for removal of phenol from aqueous solutions. Results of the effect of contact time showed that the phenol adsorption onto ARHA was rapid and obeyed the pseudo-second-order kinetic model. By increasing the values of adsorbent dose, the initial concentration of phenol, and temperature, the adsorption rate increased, decreased and decreased, respectively. Isotherm studies of phenol removal by ARHA showed that the Langmuir model best represented the adsorption data. In addition, thermodynamic studies revealed the endothermic and spontaneous nature of the adsorption process.

#### Acknowledgments

This research was a part of a research program (Project No. 391040413 in 2017) which funded by Sabzevar University of Medical Sciences, Iran. The authors gratefully acknowledge the support provided by the research center and also staff in the laboratory of health school in the university.

#### References

- [1] A.A. Al-Kahtani, S.M. Alshehri, M. Naushad, Ruksana, T. Ahamad, Fabrication of highly porous N/S doped carbon embedded with ZnS as highly efficient photocatalyst for degradation of bisphenol, *Int. J. Biol. Macromol.*, 121 (2019) 415–423.
- [2] G. Sharma, B. Thakur, M. Naushad, A.a.H. Al-Muhtaseb, A. Kumar, M. Sillanpaa, G.T. Mola, Fabrication and characterization of sodium dodecyl sulphate@iron-silico-phosphate nanocomposite: ion exchange properties and selectivity for binary metal ions, *Mater. Chem. Phys.*, 193 (2017) 129–139.
- [3] A. Kumar, M. Naushad, A. Rana, Inamuddin, Preeti, G. Sharma, A.A. Ghfar, F.J. Stadler, M.R. Khan, ZnSe- $\text{WO}_3$  nano-hetero-assembly stacked on Gum ghatti for photo-degradative removal of Bisphenol A: symbiose of adsorption and photocatalysis, *Int. J. Biol. Macromol.*, 104 (2017) 1172–1184.
- [4] Y. Yavuz, A.S. Koparal, Electrochemical oxidation of phenol in a parallel plate reactor using ruthenium mixed metal oxide electrode, *J. Hazard. Mater.*, 136 (2006) 296–302.
- [5] M.H. Dehghani, M. Mostofi, M. Alimohammadi, G. McKay, K. Yetilmezsoy, A.B. Albadarin, B. Heibati, M. AlGhouti, N. Mubarak, J. Sahu, High-performance removal of toxic phenol by single-walled and multi-walled carbon nanotubes: kinetics, adsorption, mechanism and optimization studies, *J. Ind. Eng. Chem.*, 35 (2016) 63–74.
- [6] A.D. Pereira, C.D. Leal, M.F. Dias, C. Etchebehere, C.A.L. Chernicharo, J.C. de Araújo, Effect of phenol on the nitrogen removal performance and microbial community structure and composition of an anammox reactor, *Bioresour. Technol.*, 166 (2014) 103–111.
- [7] R.W. Adler, US Environmental Protection Agency's new waters of the United States Rule: connecting law and science, *Freshwater Sci.*, 34 (2015) 1595–1600.
- [8] I. Zanotti, M. Dall'Asta, P. Mena, L. Mele, R. Bruni, S. Ray, D. Del Rio, Atheroprotective effects of (poly) phenols: a focus on cell cholesterol metabolism, *Food funct.*, 6 (2015) 13–31.
- [9] F. Shahidi, P. Ambigaipalan, Phenolics and polyphenolics in foods, beverages and spices: antioxidant activity and health effects—a review, *J. Funct. Foods*, 18 (2015) 820–897.
- [10] S. Mohammadi, A. Kargari, H. Sanaeepur, K. Abbassian, A. Najafi, E. Mofarrah, Phenol removal from industrial wastewaters: a short review, *Desal. Wat. Treat.*, 53 (2015) 2215–2234.

- [11] S. Golbaz, A.J. Jafari, M. Rafiee, R.R. Kalantary, Separate and simultaneous removal of phenol, chromium, and cyanide from aqueous solution by coagulation/precipitation: mechanisms and theory, *Chem. Eng. J.*, 253 (2014) 251–257.
- [12] S. Esplugas, J. Gimenez, S. Contreras, E. Pascual, M. Rodríguez, Comparison of different advanced oxidation processes for phenol degradation, *Water Res.*, 36 (2002) 1034–1042.
- [13] J.O. Méndez, J.H. Melián, J. Araña, J.D. Rodríguez, O.G. Diaz, J.P. Pena, Detoxification of waters contaminated with phenol, formaldehyde and phenol–formaldehyde mixtures using a combination of biological treatments and advanced oxidation techniques, *Appl. Catal., B.*, 163 (2015) 63–73.
- [14] D.P. Zagklis, A.I. Vavouraki, M.E. Kornaros, C.A. Paraskeva, Purification of olive mill wastewater phenols through membrane filtration and resin adsorption/desorption, *J. Hazard. Mater.*, 285 (2015) 69–76.
- [15] P. Shandilya, D. Mittal, M. Soni, P. Raizada, A. Hosseini-Bandegharai, A.K. Saini, P. Singh, Fabrication of fluorine doped graphene and SmVO<sub>4</sub> based dispersed and adsorptive photocatalyst for abatement of phenolic compounds from water and bacterial disinfection, *J. Cleaner Prod.*, 203 (2018) 386–399.
- [16] F. Duan, Y. Li, H. Cao, Y. Wang, J.C. Crittenden, Y. Zhang, Activated carbon electrodes: electrochemical oxidation coupled with desalination for wastewater treatment, *Chemosphere*, 125 (2015) 205–211.
- [17] S.M. Alshehri, M. Naushad, T. Ahamad, Z.A. Alothman, A. Aldalbahi, Synthesis, characterization of curcumin based ecofriendly antimicrobial bio-adsorbent for the removal of phenol from aqueous medium, *Chem. Eng. J.*, 254 (2014) 181–189.
- [18] M. Hamdaoui, M. Hadri, Z. Bencheqroun, K. Draoui, M. Nawdali, H. Zaitan, A. Barhoun, Improvement of phenol removal from aqueous medium by adsorption on organically functionalized Moroccan stevensite, *J. Mater. Environ. Sci.*, 9 (2018) 1119–1128.
- [19] M. Tanyol, Rapid malachite green removal from aqueous solution by natural zeolite: process optimization by response surface methodology, *Desal. Wat. Treat.*, 65 (2017) 294–303.
- [20] A. Mittal, M. Naushad, G. Sharma, Z. Alothman, S. Wabaidur, M. Alam, Fabrication of MWCNTs/ThO<sub>2</sub> nanocomposite and its adsorption behavior for the removal of Pb (II) metal from aqueous medium, *Desal. Wat. Treat.*, 57 (2016) 21863–21869.
- [21] G. Sharma, M. Naushad, A. Kumar, S. Rana, S. Sharma, A. Bhatnagar, F.J. Stadler, A.A. Ghfar, M.R. Khan, Efficient removal of coomassie brilliant blue R-250 dye using starch/poly(alginate-chitosan) nanohydrogel, *Process Saf. Environ. Prot.*, 109 (2017) 301–310.
- [22] G. Sharma, B. Thakur, M. Naushad, A. Kumar, F.J. Stadler, S.M. Alfadul, G.T. Mola, Applications of nanocomposite hydrogels for biomedical engineering and environmental protection, *Environ. Chem. Lett.*, 16 (2017) 1–34.
- [23] I. Anastopoulos, A. Robalds, H.N. Tran, D. Mitrogiannis, D.A. Giannakoudakis, A. Hosseini-Bandegharai, G.L. Dotto, Leaf Biosorbents for the Removal of Heavy Metals, *Green Adsorbents for Pollutant Removal*, Springer, 2018, pp. 87–126.
- [24] H.N. Tran, S.-J. You, T.V. Nguyen, H.-P. Chao, Insight into the adsorption mechanism of cationic dye onto biosorbents derived from agricultural wastes, *Chem. Eng. Commun.*, 204 (2017) 1020–1036.
- [25] A. Bhatnagar, M. Sillanpää, A. Witek-Krowiak, Agricultural waste peels as versatile biomass for water purification—a review, *Chem. Eng. J.*, 270 (2015) 244–271.
- [26] M.A. Yahya, Z. Al-Qodah, C.Z. Ngah, Agricultural bio-waste materials as potential sustainable precursors used for activated carbon production: a review, *Renewable Sustainable Energy Rev.*, 46 (2015) 218–235.
- [27] G.H. Pino, L.M. Souza de Mesquita, M.L. Torem, G.A. Saavedra Pinto, Biosorption of cadmium by green coconut shell powder, *Miner. Eng.*, 19 (2006) 380–387.
- [28] S. Ben-Ali, S. Souissi-Najar, A. Ouederni, Comments on “Comments on ‘Characterization and adsorption capacity of raw pomegranate peel biosorbent for copper removal’”, *J. Cleaner Prod.*, 154 (2017) 269–275.
- [29] R.S. Juang, R.L. Tseng, F.C. Wu, S.H. Lee, Adsorption behavior of reactive dyes from aqueous solutions on chitosan, *J. Chem. Technol. Biotechnol.*, 70 (1997) 391–399.
- [30] M.H. Salmani, M. Miri, M.H. Ehrampoush, A. Alahabadi, A. Hosseini-Bandegharai, Comparing cadmium removal efficiency of a magnetized biochar based on orange peel with those of conventional orange peel and unmodified biochar, *Desal. Wat. Treat.*, 82 (2017) 157–169.
- [31] B. Amarasinghe, Removal of Phenol from Wastewater Using Rice Husk Based Adsorbent, 2016.
- [32] H.H. Ngo, W. Guo, J. Zhang, S. Liang, C. Ton-That, X. Zhang, Typical low cost biosorbents for adsorptive removal of specific organic pollutants from water, *Bioresour. Technol.*, 182 (2015) 353–363.
- [33] P. Singh, P. Raizada, D. Pathania, G. Sharma, P. Sharma, Microwave induced KOH activation of guava peel carbon as an adsorbent for congo red dye removal from aqueous phase, *Indian J. Chem. Technol.*, 20 (2013) 305–311.
- [34] S. Khan, Z.F. Raha, M. Jabeen, M. Rukh, S.T. Reza, E.A. Khan, Removal of organic pollutant from aqueous solution by rice husk activated carbon (RHAC), *J. Chem. Eng.*, 29 (2017) 29–33.
- [35] S. Darabi, S. Fatemeh, N. Bahramifar, M.A. Khalilzadeh, Equilibrium, thermodynamic and kinetics studies on adsorption of eosin Y and red X-GRL from aqueous solution by treated rice husk, *J. Appl. Res. Wat. Wastewater*, 5 (2018) 392–398.
- [36] S.K. Hubadillah, M.H.D. Othman, Z. Harun, A. Ismail, M.A. Rahman, J. Jaafar, A novel green ceramic hollow fiber membrane (CHFM) derived from rice husk ash as combined adsorbent-separator for efficient heavy metals removal, *Ceram. Int.*, 43 (2017) 4716–4720.
- [37] C. Thakur, V.C. Srivastava, I.D. Mall, A.D. Hiwarkar, Modelling of binary isotherm behaviour for the adsorption of catechol with phenol and resorcinol onto rice husk ash, *Indian Chem. Eng.*, 59 (2017) 312–334.
- [38] P. Sudhakar, I.D. Mall, V.C. Srivastava, Adsorptive removal of bisphenol-A by rice husk ash and granular activated carbon—a comparative study, *Desal. Wat. Treat.*, 57 (2016) 12375–12384.
- [39] S. Mor, K. Chhoden, K. Ravindra, Application of agro-waste rice husk ash for the removal of phosphate from the wastewater, *J. Cleaner Prod.*, 129 (2016) 673–680.
- [40] A. Alahabadi, Z. Rezai, A. Rahmani-Sani, A. Rastegar, A. Hosseini-Bandegharai, A. Gholizadeh, Efficacy evaluation of NH<sub>4</sub>Cl-induced activated carbon in removal of aniline from aqueous solutions and comparing its performance with commercial activated carbon, *Desal. Wat. Treat.*, 57 (2016) 23779–23789.
- [41] A. Alahabadi, A. Hosseini-Bandegharai, G. Moussavi, B. Amin, A. Rastegar, H. Karimi-Sani, M. Fattahi, M. Miri, Comparing adsorption properties of NH<sub>4</sub>Cl-modified activated carbon towards chlortetracycline antibiotic with those of commercial activated carbon, *J. Mol. Liq.*, 232 (2017) 367–381.
- [42] W.E. Federation, A.P.H. Association, Standard Methods for the Examination of Water and Wastewater, American Public Health Association (APHA), Washington, DC, USA, 2005.
- [43] S. Brunauer, P.H. Emmett, E. Teller, Adsorption of gases in multimolecular layers, *J. Am. Chem. Soc.*, 60 (1938) 309–319.
- [44] V.C. Srivastava, I.D. Mall, I.M. Mishra, Characterization of mesoporous rice husk ash (RHA) and adsorption kinetics of metal ions from aqueous solution onto RHA, *J. Hazard. Mater.*, 134 (2006) 257–267.
- [45] G. Moussavi, A. Alahabadi, K. Yaghmaei, Investigating the potential of carbon activated with NH<sub>4</sub>Cl for catalyzing the degradation and mineralization of antibiotics in ozonation process, *Chem. Eng. Res. Des.*, 97 (2015) 91–99.
- [46] S.-A. Sajjadi, A. Mohammadzadeh, H.N. Tran, I. Anastopoulos, G.L. Dotto, Z.R. Lopičić, S. Sivamani, A. Rahmani-Sani, A. Ivanets, A. Hosseini-Bandegharai, Efficient mercury removal from wastewater by pistachio wood wastes-derived activated carbon prepared by chemical activation using a novel activating agent, *J. Environ. Manage.*, 223 (2018) 1001–1009.
- [47] M. Pirsahab, Z. Rezai, A. Mansouri, A. Rastegar, A. Alahabadi, A.R. Sani, K. Sharafi, Preparation of the activated carbon from India shrub wood and their application for methylene

- blue removal: modeling and optimization, *Desal. Wat. Treat.*, 57 (2016) 5888–5902.
- [48] W. Nakbanpote, B.A. Goodman, P. Thiravetyan, Copper adsorption on rice husk derived materials studied by EPR and FTIR, *Colloids Surf., A*, 304 (2007) 7–13.
- [49] N. Sarker, A. Fakhruddin, Removal of phenol from aqueous solution using rice straw as adsorbent, *Appl. Water Sci.*, 7 (2017) 1459–1465.
- [50] I.D. Mall, V.C. Srivastava, N.K. Agarwal, Removal of Orange-G and Methyl Violet dyes by adsorption onto bagasse fly ash—kinetic study and equilibrium isotherm analyses, *Dyes Pigm.*, 69 (2006) 210–223.
- [51] S. Eris, S. Azizian, Analysis of adsorption kinetics at solid/solution interface using a hyperbolic tangent model, *J. Mol. Liq.*, 231 (2017) 523–527.
- [52] M. Changmai, M. Purkait, Kinetics, equilibrium and thermodynamic study of phenol adsorption using NiFe<sub>2</sub>O<sub>4</sub> nanoparticles aggregated on PAC, *J. Water Process Eng.*, 16 (2017) 90–97.
- [53] A. Hosseini-Bandegharai, A. Allahabadi, A. Rahmani-Sani, A. Rastegar, R. Khamirchi, M. Mehrpouyan, R. Hekmat-Shoar, Z. Pajohankia, Thorium removal from weakly acidic solutions using titan yellow-impregnated XAD-7 resin beads: kinetics, equilibrium and thermodynamic studies, *J. Radioanal. Nucl. Chem.*, 309 (2016) 761–776.
- [54] Y. Li, X. Hu, X. Liu, Y. Zhang, Q. Zhao, P. Ning, S. Tian, Adsorption behavior of phenol by reversible surfactant-modified montmorillonite: mechanism, thermodynamics, and regeneration, *Chem. Eng. J.*, 334 (2018) 1214–1221.
- [55] A. Hosseini-Bandegharai, A. Alahabadi, A. Rahmani-Sani, A. Rastegar, R. Khamirchi, M. Mehrpouyan, J. Agah, Z. Pajohankia, Effect of nitrate and amine functionalization on the adsorption properties of a macroporous resin towards tetracycline antibiotic, *J. Taiwan Inst. Chem. Eng.*, 66 (2016) 143–153.
- [56] A. Gholizadeh, M. Kermani, M. Gholami, M. Farzadkia, Kinetic and isotherm studies of adsorption and biosorption processes in the removal of phenolic compounds from aqueous solutions: comparative study, *J. Environ. Health Sci. Eng.*, 11 (2013) 29–38.
- [57] A. Rahmani-Sani, R.-r. Shan, L.-g. Yan, A. Hosseini-Bandegharai, Response to "Letter to Editor: minor correction to the thermodynamic calculation using the distribution constant by Shan et al. and Rahmani-Sani et al.", *J. Hazard. Mater.*, 325 (2017) 367–368.
- [58] H.N. Tran, S.-J. You, A. Hosseini-Bandegharai, H.-P. Chao, Mistakes and inconsistencies regarding adsorption of contaminants from aqueous solutions: a critical review, *Water Res.*, 120 (2017) 88–116.
- [59] E.C. Lima, A. Hosseini-Bandegharai, J.C. Moreno-Piraján, I. Anastopoulos, A critical review of the estimation of the thermodynamic parameters on adsorption equilibria. Wrong use of equilibrium constant in the Van't Hoof equation for calculation of thermodynamic parameters of adsorption, *J. Mol. Liq.*, 273 (2019) 425–434.
- [60] P. Atkins, J. de Paula, *Physical Chemistry*, 9th ed., W. H. Freeman and Company, New York, 2010.
- [61] R. Chang, J.W. Thoman Jr., *Physical Chemistry for the Chemical Sciences*, University Science Books, Canada, 2014.
- [62] N.S. Kumar, M. Asif, M.I. Al-Hazzaa, Adsorptive removal of phenolic compounds from aqueous solutions using pine cone biomass: kinetics and equilibrium studies, *Environ. Sci. Pollut. Res.*, 25 (2018) 21949–21960.
- [63] S.-A. Sajjadi, A. Meknati, E.C. Lima, G.L. Dotto, D.I. Mendoza-Castillo, I. Anastopoulos, F. Alakhras, E.I. Unuabonah, P. Singh, A. Hosseini-Bandegharai, A novel route for preparation of chemically activated carbon from pistachio wood for highly efficient Pb (II) sorption, *J. Environ. Manage.*, 236 (2019) 34–44.
- [64] R. Khamirchi, A. Hosseini-Bandegharai, A. Alahabadi, S. Sivamani, A. Rahmani-Sani, T. Shahryari, I. Anastopoulos, M. Miri, H.N. Tran, Adsorption property of Br-PADAP-impregnated multiwall carbon nanotubes towards uranium and its performance in the selective separation and determination of uranium in different environmental samples, *Ecotoxicol. Environ. Saf.*, 150 (2018) 136–143.